MOLECULAR AND CELLULAR BIOLOGY, Apr. 2002, p. 2294–2303 Vol. 22, No. 7
0270-7306/02/$04.00+0 DOI: 10.1128/MCB.22.7.2294–2303.2002

The Ubiquitin Ligase Component Siah1a Is Required for Completion of Meiosis I in Male Mice

Ross A. Dickins,[1] Ian J. Frew,[1,2] Colin M. House,[1] Moira K. O'Bryan,[3] Andrew J. Holloway,[1] Izhak Haviv,[1] Nadia Traficante,[1] David M. de Kretser,[3] and David D. L. Bowtell[1,4]*

Peter MacCallum Cancer Institute, East Melbourne, Victoria 3002,[1] Department of Pathology[2] and Department of Biochemistry,[4] University of Melbourne, Parkville, Victoria 3010, and Monash Institute of Reproduction and Development, Monash University, Clayton, Victoria 3168,[3] Australia

Received 22 August 2001/Returned for modification 26 October 2001/Accepted 27 December 2001

The mammalian *Siah* genes encode highly conserved proteins containing a RING domain. As components of E3 ubiquitin ligase complexes, Siah proteins facilitate the ubiquitination and degradation of diverse protein partners including β-catenin, N-CoR, and DCC. We used gene targeting in mice to analyze the function of *Siah1a* during mammalian development and reveal novel roles in growth, viability, and fertility. Mutant animals have normal weights at term but are postnatally growth retarded, despite normal levels of pituitary growth hormone. Embryonic fibroblasts isolated from mutant animals grow normally. Most animals die before weaning, and few survive beyond 3 months. Serum gonadotropin levels are normal in *Siah1a* mutant mice; however, females are subfertile and males are sterile due to a block in spermatogenesis. Although spermatocytes in mutant mice display normal meiotic prophase and meiosis I spindle formation, they accumulate at metaphase to telophase of meiosis I and subsequently undergo apoptosis. The requirement of Siah1a for normal progression beyond metaphase I suggests that Siah1a may be part of a novel E3 complex acting late in the first meiotic division.

The *Drosophila melanogaster* gene *seven in absentia* (*sina*), isolated in a screen for mutations affecting *Drosophila* adult eye morphology, encodes a protein with an N-terminal RING domain (9). The *sina* mutant phenotype includes lack of R7 photoreceptor cells, sensory bristle abnormalities, reduced life span, uncoordination, and sterility. SINA interacts with a complex of proteins including Phyllopod (PHYL), EBI, and UBCD1 to promote the ubiquitination and proteasome-dependent degradation of the transcriptional repressor Tramtrack88 (TTK88) (5, 10, 12, 13, 26, 45). These findings suggest that SINA is the RING domain component of a multisubunit E3 that acts to target the degradation of TTK88 during eye development.

Highly conserved homologs of *sina* (the *Siah* genes) are found in all multicellular organisms examined, including plants. There are three functional murine *Siah* genes: *Siah1a*, *Siah1b*, and *Siah2* (11). *Siah1a* and *Siah1b* (collectively *Siah1*) encode 282-amino-acid proteins differing at only six residues. The 325-amino-acid Siah2 protein is almost identical to the Siah1 proteins except for a divergent and extended region N-terminal to the RING domain. The human genome contains only two *Siah* family genes, *SIAH1* and *SIAH2*, encoding proteins almost identical to murine Siah1a and Siah2, respectively (19, 20).

The remarkably high sequence conservation and widespread expression pattern of the mammalian Siah proteins indicate that they carry out fundamental cellular tasks. Siah proteins apparently operate in diverse signaling pathways, as they interact with several seemingly unrelated proteins. These include the guanine nucleotide exchange factor Vav (16), metabotropic glutamate receptors including mGluR1α (23), Peg3 (38), and α-tubulin (15). Other Siah-interacting proteins including Bag-1, DCC, N-CoR, c-Myb, Kid, and OBF1 are destabilized in cells overexpressing Siah (4, 15, 22, 43, 46, 47, 50). Their degradation depends on proteasome activity, indicating a role for Siah in the ubiquitin modification of interacting proteins, similar to *Drosophila* SINA. Siah interacts with UbcH5 and SUMO-1-conjugating enzyme UbcH9 (30). Therefore Siah appears to be an E3, or part of an E3 protein complex, that recruits interacting proteins to an E2 through its RING domain (21).

Several reports have implicated the *Siah* genes in cell cycle control. Expression of p53 or p21 induces *Siah1* expression in mammalian cells (1, 27, 28, 39), and *Siah1* expression causes reduced cell growth without apoptosis (31). Recent findings indicate that human SIAH1 may be an important mediator of cellular growth arrest in response to p53 expression through targeted degradation of the transcriptional activator β-catenin (28, 30; reviewed in reference 37). Consistent with the role of SIAH1 in growth arrest, serum stimulation of human fibroblasts causes a marked repression of *SIAH1* mRNA production, with kinetics similar to those of transcripts encoding proteins that inhibit the cell division cycle (24). Overexpression of SIAH1 in a human breast cancer cell line results in mitotic alterations, failed cytokinesis, and increased apoptosis, also implicating *SIAH1* in mitosis (7). These effects may be linked to the recent finding that SIAH1 interacts with and promotes the degradation of the chromokinesin Kid (15).

Despite numerous biochemical studies demonstrating a conserved E3 activity of the mammalian Siah proteins, their physiological role remains unknown. To investigate this, we pro-

* Corresponding author. Mailing address: Peter MacCallum Cancer Institute, St. Andrew's Place, East Melbourne, Victoria 3002, Australia. Phone: 61 3 9656 1296. Fax: 61 3 9656 1411. E-mail: d.bowtell@pmci.unimelb.edu.au.

duced and characterized mice with a targeted mutation of the *Siah1a* gene. The phenotype of these mice is inconsistent with many published properties of Siah proteins. The most profound cellular defect in *Siah1a* mutant mice is male sterility due to a block in spermatogenesis at metaphase of the first meiotic division, with subsequent spermatocyte apoptosis. This defines a novel function of Siah1a during meiosis.

MATERIALS AND METHODS

Targeted mutation of murine *Siah1a*. The targeting construct was built by using the pPNT vector (49). DNA obtained from screening a 129sv genomic library (11) was subcloned into plasmids and used to generate the 5′ and 3′ targeting arms (see Fig. 1A). A 2.5-kb *Kpn*I fragment from immediately 5′ of the *Siah1a* coding sequence was cloned into the *Kpn*I site of pPNT between the *neo* and thymidine kinase genes, and its orientation was checked by restriction digestion. To generate the 3′ arm, a parental 7.8-kb *Bam*HI/*Kpn*I genomic DNA fragment in pBluescript (no. 1513) was used. To generate more polylinker sites, the 3′ 7.0 kb of this fragment was shuttled in two steps into pHXK, derived from pHSS (42). First, a 3.0-kb (*Bst*XI)/*Sac*I fragment from 1513 was cloned into (*Sal*I)/*Sac*I-digested pHXK (parentheses indicate that the restriction endonuclease site is blunted). The resultant plasmid was digested with *Sac*I/*Kpn*I, and the adjacent 4.0-kb *Sac*I/*Kpn*I fragment from 1513 was inserted. From this, the 3′ arm was isolated as a 7.0-kb (*Bam*HI)/*Not*I fragment and cloned into (*Xho*I)/*Not*I-digested 5′ arm-pPNT. After verification with restriction enzymes, the construct was amplified and purified twice through CsCl gradients.

Fifteen micrograms of *Not*I-linearized construct was electroporated into W9.5 129sv embryonic stem (ES) cells, which were cultured on a fibroblast feeder layer. Colonies were selected in media containing 10^3 U of leukemia inhibitory factor (Amrad)/ml, 200 μg of G-418 (GibcoBRL)/ml, and 2 μM ganciclovir (Syntex). Genomic DNA from resistant colonies was digested with *Bst*XI and Southern blotted (41). Blots were probed with an 800-bp *Kpn*I fragment (probe P) from immediately upstream of the *Kpn*I site marking the 5′ end of construct homology, producing a 5.2-kb band for wild-type clones and an additional 4.4-kb band for targeted clones. Targeted ES cells (clones 12E5 and 3A4) were injected into C57BL/6J blastocysts to generate chimeras, which were mated to C57BL/6J females. Agouti pups were genotyped, and heterozygotes were intercrossed to generate *Siah1a*$^{-/-}$ mice. To confirm deletion of the coding region, a Southern blot of *Sac*I-digested genomic DNA of each genotype was probed with a 560-bp *Ssp*I fragment from the coding region of the *Siah1b* gene. Further genotyping was done by PCR using the primers 1afwd (5′GCGAATTCCAAGTATCTATGAC ATGTATA), 2005 (5′TGGACTTGTGCTGATGC), and 409 (5′GAAGAACG AGATCAGCAGCCTCTGTTCCAC). 1afwd and 2005 yield a 560-bp fragment from the wild-type allele, whereas 1afwd and 409 yield a 285-bp fragment from the targeted allele. PCR conditions were 38 cycles of 20 s at 95°C, 30 s at 57°C, and 40 s at 72°C. Phenotypic data were obtained by using mice with a mixed (C57BL/6J × 129sv) genetic background; however, the mutant phenotype was recapitulated in pure 129sv mice, derived from either the 12E5 or 3A4 ES clones (data not shown).

Northern and Western blot analyses. mRNA was isolated from the testes, brains, and spleens of each genotype. Northern blots were hybridized with the same probe used for the coding region Southern blot. Mouse organ protein lysates were prepared in radioimmunoprecipitation buffer (25 mM Tris [pH 8], 50 mM NaCl, 0.5% NP-40, 0.5% sodium deoxycholate, 0.1% sodium dodecyl sulfate [SDS]) containing 1 μg of pepstatin, 10 μg of leupeptin, and 10 μg of aprotinin/ml; 1 mM phenylmethylsulfonyl fluoride; and 50 μM MG132 proteasome inhibitor. Samples were assayed for protein content with Bradford reagent, and 25 to 75 μg of protein was separated by reducing SDS-polyacrylamide gel electrophoresis. Following Western transfer, filters were probed with monoclonal anti-Siah1 antibody 3A9 at 5 μg/ml, a rabbit anti-Kid antibody at 6 μg/ml, or a goat anti-SCP3 antibody at 1:150. Anti-Siah monoclonal antibodies were produced by immunizing mice with the full-length Siah1 protein.

Histological analysis. Testes were fixed in Bouin's solution, dehydrated, and embedded in paraffin wax. Sections were stained with hematoxylin and eosin. Immunohistochemistry was performed with an LSAB+ kit with 3,3′-diaminobenzidine chromogen (DAKO). In situ labeling of apoptotic cells was carried out using the ApopTag Plus peroxidase kit (Intergen). For transmission electron microscopy, mice were anesthetized and testes were fixed by perfusion using 4% paraformaldehyde and 5% glutaraldehyde in 80 mM Sorensen's phosphate-buffered saline. Testes were processed and sectioned by standard procedures.

Meiotic prophase analysis. Chromosome spreads were prepared based on previously described methods (36). Briefly, a germ cell suspension was made in alpha-modified Eagle's medium with 25 mM glucose. After pelleting and resuspension in 0.1 M sucrose buffered with 10 mM boric acid, pH 9.2, a drop of germ cells was gently added to a film of 1% paraformaldehyde, pH 9.2, on a clean glass slide. Slides were incubated for 2 h in a humid chamber, rinsed with 0.4% Agepon (Agfa), and stored frozen.

Primary antibodies used for indirect immunofluorescence were goat anti-SCP3 at 1:200, monoclonal anti-α-tubulin (Sigma) at 15 μg/ml, monoclonal anti-SUMO-1 (Zymed) at 3 μg/ml, and rabbit anti-Kid at 8 μg/ml. Secondary antibodies used were Alexa488 donkey anti-goat immunoglobulin G (IgG) and Alexa594 rabbit anti-mouse IgG (Molecular Probes) and Cy3 donkey anti-rabbit IgG (Jackson ImmunoResearch). DNA was stained with DAPI (4′,6′-diamidino-2-phenylindole). Slides were examined with a Zeiss Axioskop 2 microscope, and images were captured by a Diagnostic Instruments SPOT camera and manipulated with Adobe Photoshop software.

Hormone assays. Follicle-stimulating hormone (FSH) and luteinizing hormone (LH) concentrations were determined by radioimmunoassay, with reagents provided by the National Institute of Diabetes and Digestive and Kidney Diseases (Bethesda, Md.). Tracer hormone iodinations were carried out using Iodo-Gen reagent (Pierce). The lower limits of detection of FSH and LH were 0.33 and 0.11 ng/ml, respectively. The within-assay variations in the FSH and LH assays were 7.4 and 5.1%, respectively. Testosterone concentrations were measured by direct radioimmunoassay as described previously (35).

RESULTS

Production of *Siah1a* mutant mice. The *Siah1a* coding region resides on a single exon. A targeting construct was designed to replace the coding region with a neomycin resistance cassette (*neo*), leaving only the first 22 codons intact (Fig. 1A). Gene targeting was achieved in 20 of 650 G-418-resistant ES cell clones (see Materials and Methods). Germ line-transmitting chimeras yielded *Siah1a* heterozygotes, which were intercrossed to produce progeny of all three genotypes (Fig. 1B). Southern analysis, using a probe that hybridizes to each *Siah1* gene (11), demonstrated specific loss of the 4.3-kb *Siah1a*-hybridizing band in *Siah1a*$^{+/-}$ and *Siah1a*$^{-/-}$ mice (Fig. 1C).

Northern analysis of brain and testis mRNA, using a probe that detects *Siah1a* and *Siah1b* transcripts, demonstrated that the two differentially polyadenylated *Siah1* transcripts (11) were reduced in the brains, and almost completely absent in the testes, of *Siah1a*$^{-/-}$ mice (Fig. 1D). The remaining signal presumably represents *Siah1b* mRNA. *Siah2* transcript levels, normally low in testis (11), were unaffected by *Siah1a* mutation (data not shown).

Lysates from testes and brain were Western blotted with a monoclonal antibody recognizing Siah1 that we generated (Fig. 1E). Two specific protein species were detected in testes of wild-type and *Siah1a*$^{+/-}$ mice, one of the predicted size for Siah1 proteins (33 kDa) and another of 64 kDa. *Siah1a* mutation resulted in loss of over 90% of both species, suggesting that the larger species may be a modified Siah1 protein. As the targeted allele lacks the *Siah1a* coding region, the remaining Siah1 protein observed is presumably Siah1b.

Siah1a deficiency causes postnatal growth retardation and mortality. Disruption of *Siah1a* caused postnatal growth retardation. The weight and morphology of embryonic day 18.5 (e18.5) *Siah1a*$^{-/-}$ embryos were normal; however, *Siah1a*$^{-/-}$ pups weighed significantly less than their littermates 24 h after birth (data not shown). This continued throughout postnatal development, and adult mutant mice were consistently about 60% of normal weight (Fig. 2A and B). Externally, *Siah1a*$^{-/-}$ mice were normally proportioned, and carcass weight was de-

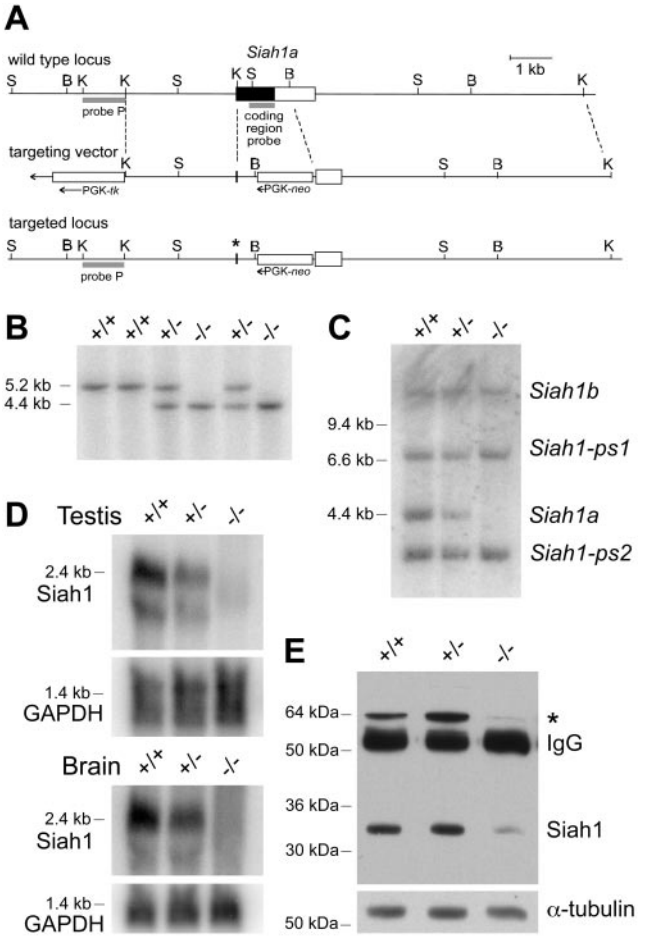

FIG. 1. Disruption of *Siah1a* by gene targeting. (A) Targeting strategy Box, single coding exon of the wild-type *Siah1a* locus (coding region is black). The targeting vector is shown below the wild-type locus, with parallel dashed lines bordering the targeting sequences. Homologous recombination yields the targeted locus, containing only the first 22 codons of the *Siah1a* coding region (*). B, *Bst*XI; K, *Kpn*I; S, *Sac*I. (B) Southern analysis of *Bst*XI-digested genomic DNA from progeny of a $Siah1a^{+/-}$ intercross. Probe P hybridizes to a region 5′ of the targeting sequence and was used to distinguish between the wild-type (5.2-kb) and targeted (4.4-kb) alleles. (C) Southern analysis of *Sac*I-digested genomic DNA from progeny of a $Siah1a^{+/-}$ intercross, probed with a coding region fragment that hybridizes to the four murine *Siah1* genes including pseudogenes *Siah1-ps1* and *Siah1-ps2*. (D) Northern blot of mRNA isolated from testes and brains of mutant and control mice and hybridized with the *Siah1* coding region fragment used for Southern analysis. Blots were stripped and reprobed with a GAPDH (glyceraldehyde-3-phosphate dehydrogenase) loading control. (E) Western blot of whole-testis lysates from mutant and control mice, blotted with anti-Siah1 monoclonal antibody 3A9. *, 64-kDa species.

creased in proportion to body weight. The sizes of the gastrointestinal tracts and most other organs of $Siah1a^{-/-}$ mice relative to total body weight were also normal; however, the testes and livers were disproportionately small (Fig. 2C). Although lower than those of littermate controls, brain and lung weights were disproportionately increased relative to body size in $Siah1a^{-/-}$ mice. We measured the abundances of Siah target proteins β-catenin and Bag-1 in spleens, thymuses, large intestines, kidneys, livers, testes, lungs, brains, and skeletal muscles of control and $Siah1a^{-/-}$ mice by Western analysis. No differences in the steady-state levels of these proteins were observed (Fig. 2D). Available antibodies to other Siah substrates were ineffective. In addition, blotting with an anti-Siah1 monoclonal antibody revealed that Siah1b protein was present at low levels in all $Siah1a^{-/-}$ tissues examined, and its abundance relative to that of the wild-type total Siah1 protein was constant for most tissues (Fig. 2D).

To test whether cell cycle abnormalities were the basis of the growth phenotype, we compared growth of murine embryonic fibroblasts (MEFs) derived from wild-type embryos and $Siah1a^{-/-}$ embryos. Early-passage $Siah1a^{-/-}$ MEFs grew at a normal rate in culture and underwent senescence equivalently to wild-type cells (Fig. 3A and B). The ratio of cells in each phase of the cell cycle was also normal (Fig. 3C). These data suggested that the growth defect of $Siah1a^{-/-}$ mice was unlikely to be a result of reduced cell proliferation.

The postnatal smallness and sterility (see below) of mutant mice indicated a possible defect in development of the anterior pituitary gland, which produces the gonadotropins and growth hormone (GH). However GH levels in whole-pituitary lysates from mutant animals were normal (control mice, 22.8 ± 2.1 ng/mg of pituitary tissue [$n = 6$]; $Siah1a^{-/-}$ mice, 18.9 ± 3.7 ng/mg [$n = 5$]; means ± standard errors of the means). *Siah1a* maps closely to the *proportional dwarf* (*pdw*; [44]) mutation on mouse chromosome 8 (19), but sequencing the *Siah1a* coding region of *pdw* mice failed to detect any mutations (data not shown). We have not tested whether *pdw* is allelic to *Siah1a* by intercrossing.

Siah1a deficiency also caused premature death. The genotypes of embryos and newborn litters from $Siah1a^{+/-}$ intercrosses conformed to the predicted Mendelian ratio (21 +/+:56 +/−:26 −/− or 1:2.7:1.2). However, this ratio was 85:152:24 (1:1.8:0.3) for pups at weaning; thus, about 70% of $Siah1a^{-/-}$ pups died during the nursing period. Increased mortality also occurred in older $Siah1a^{-/-}$ mice, sometimes associated with wasting, but some survived several months. Life span was improved by providing a food slurry, but many animals died at an apparently healthy weight. To check for potential causes of death, all vital organs were histologically surveyed; however, no major abnormalities were uncovered. Despite their unusually small size, livers from several $Siah1a^{-/-}$ mice showed no evidence of increased apoptosis, as measured by terminal deoxynucleotidyltransferase-mediated dUTP-biotin nick end labeling (TUNEL) staining (data not shown). Hematopoietic tissues appeared normal in $Siah1a^{-/-}$ mice, as judged by histology and flow cytometry of T-cell, B-cell, and granulocyte lineages.

Mutant male sterility and female subfertility. When mated to wild-type females, $Siah1a^{-/-}$ males were infertile. $Siah1a^{-/-}$ testes were disproportionately small (Fig. 2C), despite normal serum testosterone levels (control mice, 5.4 ± 3.4 ng/ml [$n = 11$]; $Siah1a^{-/-}$ mice, 11.6 ± 4.8 ng/ml [$n = 11$]). Furthermore the levels of FSH and LH in serum and whole-pituitary lysate from mutant mice of both sexes and controls were not significantly different (data not shown), indicating that the pituitary gonadal axis was intact.

Several $Siah1a^{-/-}$ female mice were mated to wild-type males. Litters were produced infrequently, only by particular females, and died within 1 day. Ovarian follicles appeared

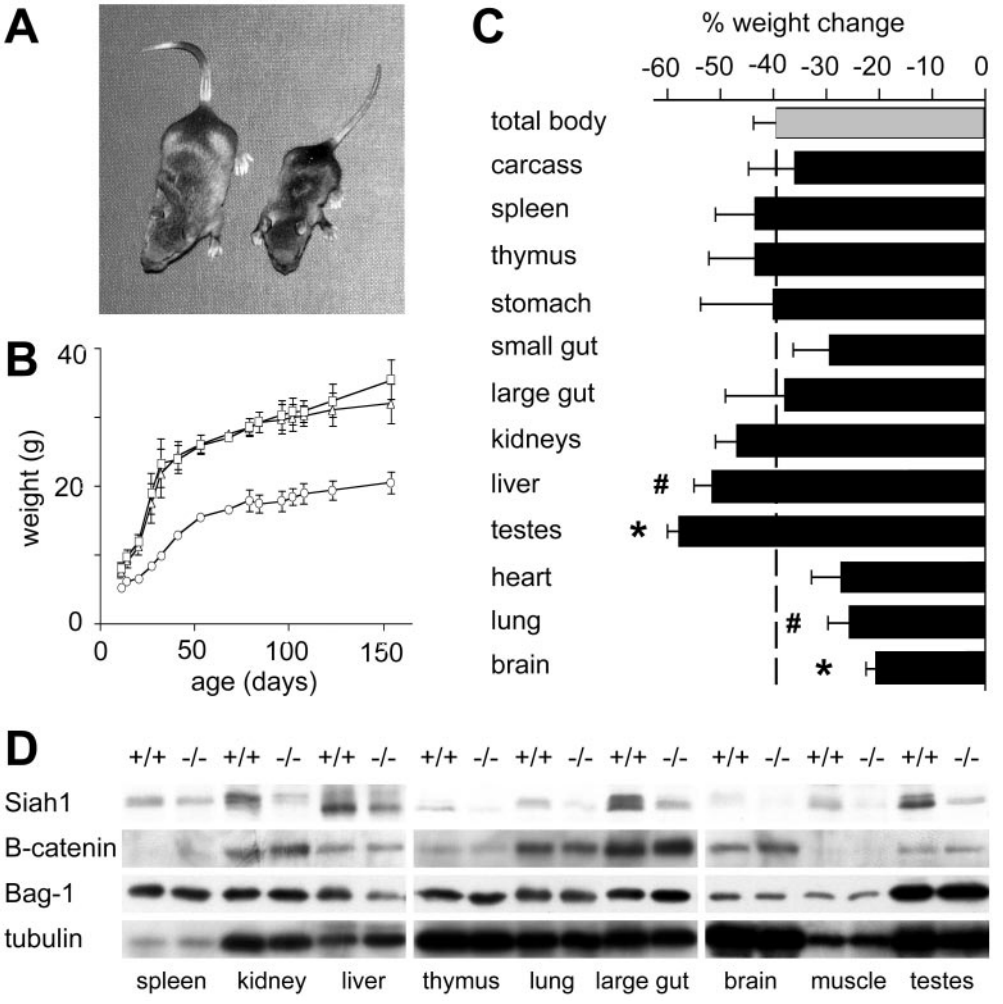

FIG. 2. *Siah1a*$^{-/-}$ mice are growth retarded. (A) Small size of a 2-week-old *Siah1a* mutant mouse (right) compared to that of a sex-matched wild-type littermate (left). (B) Representative growth curve (means and ranges) of male *Siah1a*$^{+/+}$ (squares; $n = 2$), *Siah1a*$^{+/-}$ (triangles; $n = 4$), and *Siah1a*$^{-/-}$ (circles; $n = 2$) mice from two age-matched litters. Data for females showed a similar trend. (C) Wet weights (means ± standard errors of the means) of tissues from *Siah1a*$^{-/-}$ animals expressed as percent changes compared to those of wild-type littermates. Data were obtained from mice between 3 and 10 weeks of age ($n = 7$ to 10; $n = 16$ for testes). *, $P < 0.001$; #, $P < 0.05$ (both compared to change in total body weight (grey). (D) Western blot of organ lysates from mutant and control mice, blotted with antibodies recognizing Siah1, β-catenin, and Bag-1.

histologically normal, and *Siah1a*$^{-/-}$ female fertility is not examined here.

Interrupted spermatogenesis in *Siah1a* mutant males. Spermatogenesis occurs in the seminiferous tubules of the testes. Spermatogonia in the basal region of tubules undergo mitosis to form spermatocytes, which undergo a premeiotic S phase and a lengthy meiotic prophase. Two rapid meiotic divisions without an intervening S phase form haploid spermatids, which elongate and are eventually released into the tubule lumen as immature spermatozoa (Fig. 4A). This process is highly ordered and occurs in waves along a seminiferous tubule; therefore, a single testis section allows examination of tubules at each stage of spermatogenesis (40).

Testes from adult *Siah1a*$^{-/-}$ mice displayed gross defects of the seminiferous tubule epithelium, varying in severity among males (Fig. 4). Intertubular regions, Sertoli cells, and spermatogonia all appeared normal. However postmeiotic round and elongating spermatids were completely absent in about one-half of the mutant mice examined (Fig. 4C and E), and severely depleted in the remainder (Fig. 4F). Phenotypic heterogeneity was observed even on a pure 129sv genetic background.

Spermatocytes in prophase I of meiosis in *Siah1a*$^{-/-}$ mice appeared normal; however, spermatocytes undergoing the meiotic divisions were abnormal. In males with a more marked phenotype, progression past meiotic metaphase I was rare, and all cells at anaphase I or beyond appeared unusual. Defects included degeneration of metaphase and anaphase cells (Fig. 4C and G to I) and bi- or multinucleated cells, indicating failure to complete chromosome segregation and meiotic division (Fig. 4C and I). The seminiferous epithelium was vacuolated, and immature germ cells were present in the lumen (Fig. 4C and E). Consequently the mutant epididymis was devoid of spermatozoa and contained only immature spermatocytes,

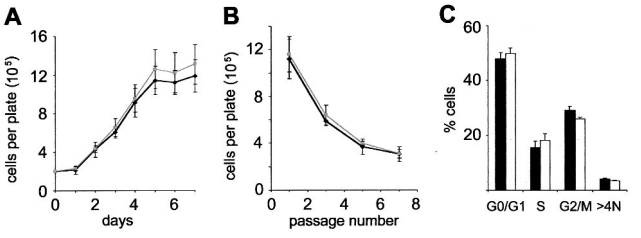

FIG. 3. Growth properties of *Siah1a*$^{-/-}$ MEFs. Means ± standard deviations (*Siah1a*$^{+/+}$embryos, $n = 2$; *Siah1a*$^{-/-}$ embryos, $n = 3$) from duplicate assays of each of n independent MEF preparations derived from littermate e14 embryos are shown. Similar results were obtained with MEFs derived from separate litters. Black, wild type; grey (A and B) or white (C), *Siah1a*$^{-/-}$. (A) MEF growth. Passage 4 MEFs were plated at 2×10^5 cells/60-mm-diameter culture dish, and cell numbers were determined daily for 7 days. (B) 3T3 analysis of MEF proliferation and senescence. Passage 4 MEFs were plated at 3×10^5 cells/60-mm-diameter culture dish. Cell numbers were determined after 3 days, before replating at the starting density. MEFs of both genotypes underwent senescence by passage 7. (C) Cell cycle distribution of asynchronously growing passage 4 MEFs. Flow cytometry using 5-bromo-2′-deoxyuridine labeling and propidium iodide staining was used to assess the percentage of cells in each phase of the cell cycle.

many with compacted chromatin and apparently in the process of meiotic division or degeneration (Fig. 4K).

In mice, the first wave of spermatogenesis begins shortly after birth, the first meiotic divisions occur at about postnatal day 20 (p20), and by p35 the first spermatozoa are produced (32). We examined testes of *Siah1a*$^{-/-}$ animals at specific developmental stages. At p18, spermatocytes were the most mature germ cells in wild-type and *Siah1a*$^{-/-}$ mice (Fig. 4L and M). However by p22, when most wild-type tubules contained postmeiotic round spermatids (Fig. 4N), *Siah1a*$^{-/-}$ testes were clearly abnormal. Round spermatids were absent; however, many tubules contained dividing spermatocytes or were vacuolated due to spermatocyte loss (Fig. 4O). These findings suggested that neither mitotic proliferation of spermatogonia nor meiotic prophase was compromised in *Siah1a*$^{-/-}$ mice; however, progression beyond metaphase I was defective.

***Siah1a* deficiency impairs progression past meiotic metaphase I.** Spermatocytes undergoing the meiotic divisions are distinguishable from prophase spermatocytes by their chromatin morphology. Examination of every tubule (approximately 300) in a testis midline section from 10-week-old animals revealed that 13.5 ± 2.1% of *Siah1a*$^{-/-}$ mouse tubules harbored meiotically dividing spermatocytes compared to 8.3 ± 1.4% for littermate controls ($n = 5$; $P < 0.05$), suggesting that the process of meiotic cell division was slightly prolonged in *Siah1a*$^{-/-}$ spermatocytes. The prophase of meiosis lasts about 3 weeks in mice and consists of four main stages: leptonema, zygonema, pachynema, and diplonema. As spermatogenesis progresses from stage XII to stage I, spermatocytes complete both meiotic divisions to form round spermatids and within the same tubule zygotene spermatocytes enter pachynema (40). In *Siah1a*$^{-/-}$ testes, dividing spermatocytes persisted in stage I tubules (data not shown), consistent with delayed progression through the meiotic cell division cycle. Many of these accumulating spermatocytes remained at metaphase I.

The prolonged metaphase I and lack of postmeiotic cells in *Siah1a*$^{-/-}$ testes prompted an investigation of germ cell death using TUNEL staining. Apoptotic spermatocytes were abundant in particular seminiferous tubules in *Siah1a*$^{-/-}$ testis sections, indicating stage-specific cell death (Fig. 5B). Invariably these tubules harbored meiotically dividing cells, and many degenerating spermatocytes appeared to be stalled at metaphase I. Other dying cells showed chromatin separation reminiscent of anaphase, were binucleated, or appeared to be at metaphase II (Fig. 5C to E). Tubules containing only prophase I spermatocytes were not TUNEL positive (Fig. 5B). Not all tubules containing metaphase I spermatocytes were TUNEL positive, presumably because these cells had not been delayed for sufficient time to trigger apoptosis. Germ cell apoptosis in p18 *Siah1a*$^{-/-}$ testes (Fig. 5F) was minimal and comparable with that in testes of p18 or p22 wild-type mice. However widespread apoptosis of dividing spermatocytes was observed within particular tubules of p22 mutant testes (Fig. 5G). Together with data from adult mice, this suggested that *Siah1a*$^{-/-}$ germ cells either underwent apoptosis at metaphase I or progressed to anaphase or telophase I before degenerating.

Normal meiotic prophase and spindle assembly in *Siah1a* mutant germ cells. We initially hypothesized that failure to properly progress past meiotic metaphase I may be caused by activation of a checkpoint, as has been observed in mice with defective pairing of homologous chromosomes (homologs) during prophase (see Discussion). We examined homolog synapsis and recombination in *Siah1a*$^{-/-}$ spermatocytes using whole-testis germ cell spreading. Prophase progression was monitored by indirect immunofluorescence staining of SCP3 (25), which is part of the synaptonemal complex between synapsed homologs during pachynema and remains on the desynapsed axes during diplonema. No abnormalities in chromosome pairing were detected in *Siah1a*$^{-/-}$ spermatocytes, by either SCP3 staining or electron microscopy of synaptonemal complexes (Fig. 6A to E). The ratio of pachytene to diplotene spermatocytes in *Siah1a*$^{-/-}$ spreads was normal, as were sex chromosome pairing, the number of chiasmata per diplotene bivalent, and the localization of other recombination proteins such as RAD51 and MLH1 (data not shown). Collectively all stages of meiotic prophase in *Siah1a*$^{-/-}$ mice appeared normal.

Accumulation of metaphase I spermatocytes in *Siah1a*$^{-/-}$ testes also suggested possible activation of a meiosis I spindle checkpoint; however, normal bipolar meiosis I spindles were observed (Fig. 6F). In addition, costaining of α-tubulin and SCP3, which remains on kinetochores until anaphase II (33), revealed normal microtubule attachment to kinetochores in the majority of *Siah1a*$^{-/-}$ spermatocytes examined (Fig. 6H).

Kid expression during mammalian meiosis I. The accumulation and death of *Siah1a*$^{-/-}$ spermatocytes at metaphase to telophase I were consistent with failed degradation of an anaphase I inhibitor protein, and we hypothesized that Siah1a may be required for Kid proteolysis at metaphase I (see Discussion). Kid localizes to the mitotic spindle and chromatin in somatic cells (48), but its role in meiosis I was unknown. Using immunofluorescence we found that in both wild-type and *Siah1a*$^{-/-}$ spermatocytes Kid was present on chromatin during meiotic prophase (Fig. 6I) and also on the meiosis I spindle

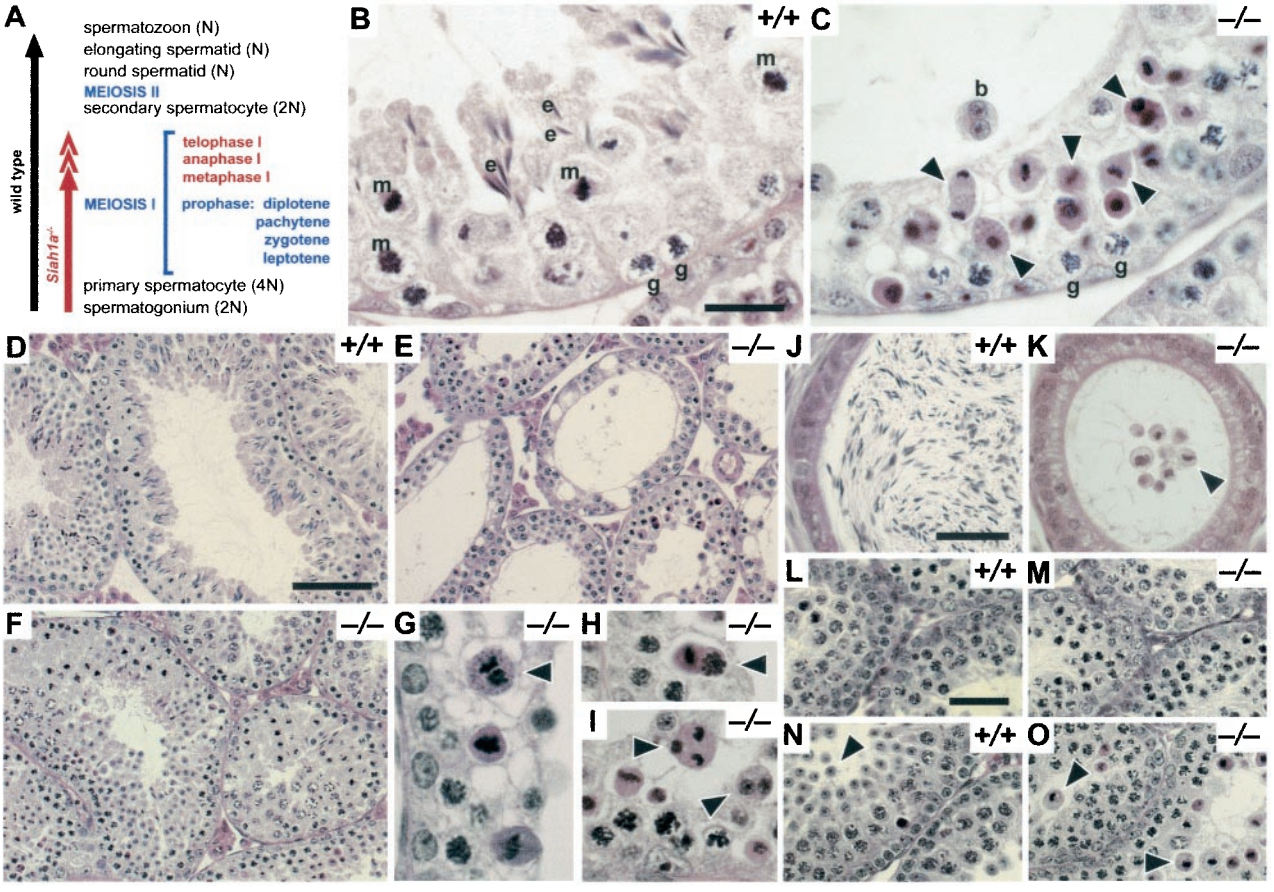

FIG. 4. Defective spermatogenesis in *Siah1a*$^{-/-}$ mice. (A) Schematic of spermatogenesis, including the stages of meiosis I where *Siah1a*$^{-/-}$ spermatogenesis is clearly aberrant (red). Not all cell types listed are present in a single seminiferous tubule section. (B to O) Hematoxylin- and eosin-stained testis and epididymis sections from representative *Siah1a*$^{-/-}$ and control mice. (B to I) Testis sections from adult mice. (B) Wild type at stage XII (40), showing spermatogonia (g), metaphase I spermatocytes (m), and elongating spermatids (e). (C) Severely affected *Siah1a*$^{-/-}$ testis at a stage similar to that shown in panel B but with clearly abnormal dividing spermatocytes at metaphase through telophase I (arrowheads). Note the abnormally eosinophilic cytoplasm of degenerating dividing spermatocytes, a binucleated spermatid (b), and the absence of elongating spermatids. (D to F) Normal testis morphology of wild-type mice (D) compared to the complete or partial absence of postmeiotic cells in mutants with severe (E) or mild (F) phenotypes. (G to I) Abnormal spermatocytes in mutant animals. Defects observed include apparently degenerating metaphase and anaphase I spermatocytes (G and H; arrowheads) and unusual chromatin figures and binucleated cells (I, arrowheads). (J and K) Epididymis sections showing abundant spermatozoa in the wild type (J) compared to mutant (K), which contains only immature spermatocytes. Many of these have chromatin figures reminiscent of meiotically dividing cells (arrowhead). (L to O) Testis sections from wild-type (L and N) and mutant (M and O) juvenile mice. At day 18 (L and M) the wild type and mutant are comparable. By day 22 (N and O) round spermatids are present in the wild type (arrowhead); however *Siah1a*$^{-/-}$ tubules harbor abnormal spermatocytes undergoing meiotic division (arrowhead). Bars: 10 (B, C, and G to I), 50 (D to F), and 20 μm (J to O).

(Fig. 6J and K). However we were unable to discern differences in Kid abundance between *Siah1a*$^{-/-}$ cells and controls. In addition, no consistent difference in the abundance of Kid was found by Western analysis of testis lysates when results were normalized against those for meiotic antigen SCP3 (Fig. 6L).

DISCUSSION

Siah1a is required for male meiosis I. We have described a novel function of Siah1a in meiosis. The initiation and duration of meiotic prophase in *Siah1a*$^{-/-}$ mice are normal; however, spermatocytes appear to accumulate at metaphase I prior to apoptosis. Although some spermatocytes apparently progress beyond metaphase I, they appear abnormal and fail to divide. Metaphase arrest, caused by failed meiotic recombination (3) or sex chromosome asynapsis (8, 29), has been observed in other mutant mice. Despite strong histological similarities between these mice and *Siah1a*$^{-/-}$ animals, we were unable to detect homolog asynapsis or other meiotic prophase abnormalities in *Siah1a*$^{-/-}$ spermatocytes.

Possible targets of Siah1a E3 activity during meiosis I. Siah proteins function biochemically as E3 ubiquitin ligase components, so it is probable that the block at meiosis I in *Siah1a*$^{-/-}$ spermatocytes is due to perturbed proteolysis of one or more substrates of Siah1a. As meiosis stalls at metaphase I through telophase I but not before, Siah1a may play a role in the metaphase I-to-anaphase I transition. Ubiquitin-dependent proteolytic cleavage of anaphase inhibitors facilitates the metaphase-to-anaphase transition in cell division across all species (reviewed in reference 34). The separase inhibitor securin ap-

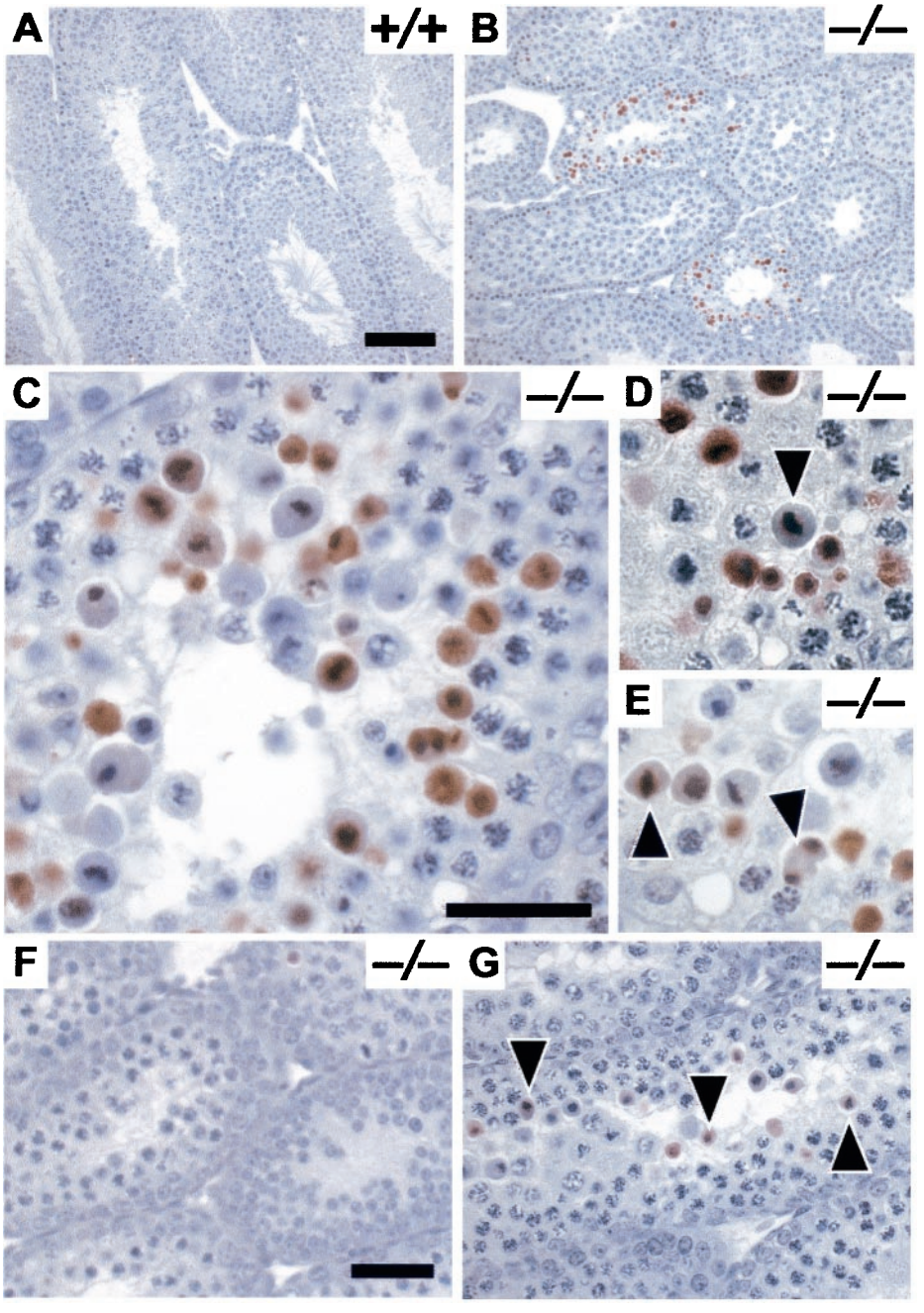

FIG. 5. In situ staining of apoptotic spermatocytes in mutant testes. DNA fragmentation was visualized by TUNEL staining (hematoxylin counterstained). (A to E) Adult testes from wild-type (A) and mutant (B to E) mice. Apoptosis in mutants is confined to particular seminiferous tubules (B), all containing meiotically dividing spermatocytes (C). Apoptotic DNA fragmentation (D and E) is clearly visible in spermatocytes at metaphase I to telophase I (arrowheads). (F and G) Developmental analysis of apoptosis in testis from *Siah1a*$^{-/-}$ mice at days 18 (F) and 22 (G). Note the appearance of numerous apoptotic spermatocytes (arrowheads) at day 22. Bars: 50 (A and B), 10 (C to E), and 20 μm (F and G).

pears unlikely to be a target of Siah1a at metaphase I, because disjunction of homologs is observed in many mutant spermatocytes. Recent studies have revealed a second inhibitor of chromosome segregation, the Kid chromokinesin (reviewed in reference 17). Human Kid is a microtubule-associated motor protein that binds DNA, and during mitosis Kid is found on chromosomes and the spindle (48). A *Xenopus* homolog of Kid (Xkid) is required for metaphase chromosome alignment in frog egg extracts (2, 14). Xkid is rapidly degraded at anaphase, and inhibiting its degradation prevents anaphase onset. Therefore Xkid provides a polar ejection force on chromosomes that must be inactivated to allow their segregation. In the *Xenopus* egg extract system, which reconstitutes meiosis II, Xkid proteolysis at anaphase requires anaphase-promoting complex/cyclosome activity (14). However human Kid was recently found to interact with human SIAH1, and overexpression of SIAH1

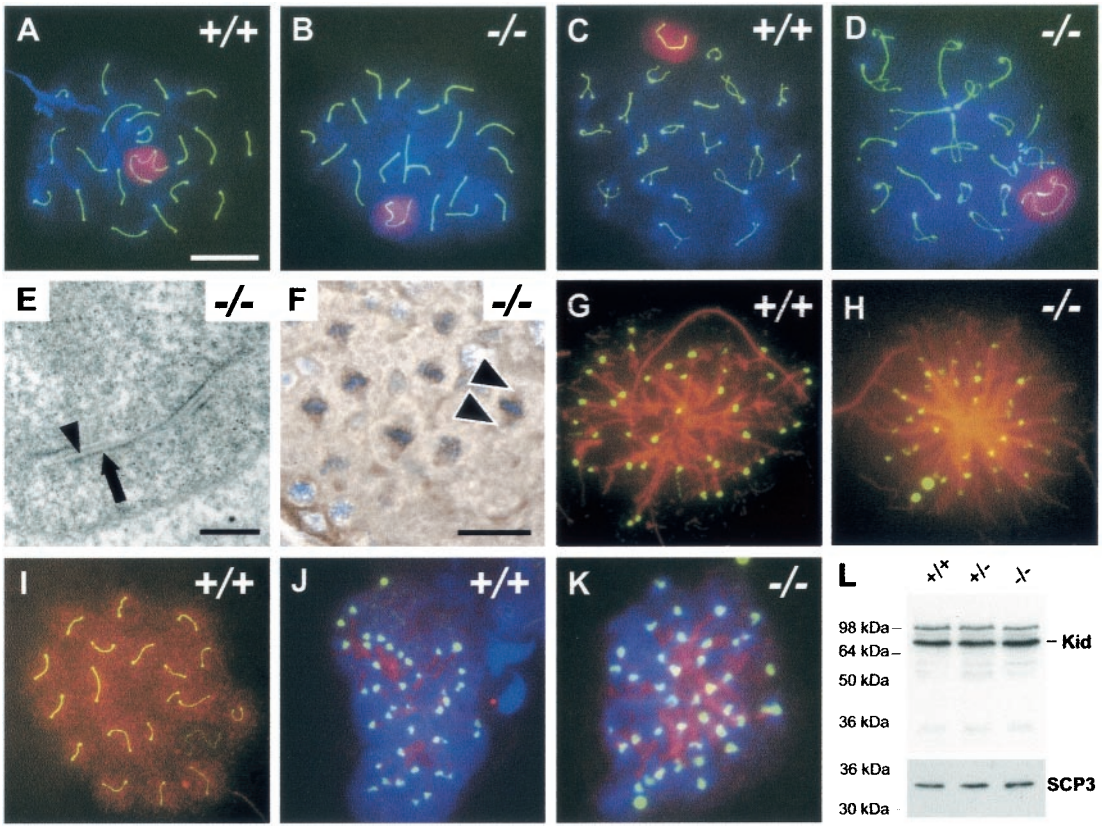

FIG. 6. Meiotic prophase analysis and Kid expression in mutant spermatocytes. Thousands of spermatocytes from several wild-type and *Siah1a*$^{-/-}$ mice exhibiting various degrees of phenotypic severity were examined. Typical cells are shown. (A to D) Spermatocytes from wild type (A and C) and *Siah1a*$^{-/-}$ (B and D) germ cell spreads stained with DAPI to visualize DNA (blue) and antibodies to SCP3 (green) and SUMO-1 (red). SUMO-1 localizes to the sex body, allowing identification of the paired X and Y chromosomes. (A and B) Pachytene spermatocytes showing 19 fully synapsed autosomal bivalents and an X-Y chromosome pair. (C and D) Diplotene spermatocytes showing normal chiasma formation and end-to-end X-Y chromosome attachment. (E) Transmission electron micrograph of a *Siah1a*$^{-/-}$ pachytene spermatocyte. The synaptonemal complex is morphologically normal; lateral (arrow) and central (arrowhead) elements are indicated. (F) Anti-α-tubulin immunohistochemistry showing normal spindle morphology (arrowheads) in *Siah1a*$^{-/-}$ metaphase I spermatocytes. (G and H) Metaphase I spermatocytes from wild-type (G) and *Siah1a* mutant (H) mice stained with DAPI and antibodies to SCP3 (green) and α-tubulin (red). Each spermatocyte has settled down flat, collapsing on its spindle pole axis. Thus bipolar spindle morphology is not seen but kinetochores are easily distinguishable. Each of the 40 SCP3 foci represents a superimposed pair of sister kinetochores (6), corresponding to the diploid chromosome number. Kinetochore attachment and spindle morphology in wild-type spermatocytes are comparable to those in *Siah1a*$^{-/-}$ spermatocytes. (I to L) Kid expression in mammalian spermatocytes. (I to K) Spermatocytes from wild-type (I and J) and *Siah1a*$^{-/-}$ (K) germ cell spreads stained with antibodies to SCP3 (green) and Kid (red). Metaphase I spermatocytes (J and K) are also stained with DAPI (blue). Kid localizes to chromatin in prophase spermatocytes (I) and to the metaphase I spindle in spermatocytes of both genotypes (J and K). (L) Western blot of whole-testis lysates from mutant and control mice, blotted with the anti-Kid antibody. Kid migrates at approximately 70 kDa. Bars: 5 (A to D, G, H, and I to K), 1 (E), and 10 μm (F).

in cells causes ubiquitin-dependent Kid degradation (15). Therefore Kid protein levels may be regulated by more than one E3 ubiquitin ligase complex.

The inability of many *Siah1a*$^{-/-}$ spermatocytes to enter anaphase I is consistent with persistence of a polar ejection force acting on chromosomes, and it is tempting to speculate that accumulation of the Kid protein may be the basis for this. The role of Kid during meiosis I was not known. We demonstrate that Kid localizes to the metaphase I spindle, consistent with a role for Kid in meiosis I chromosome movement. However it is not known whether Kid degradation is necessary for chromosome segregation at anaphase I. We have been unable to observe an accumulation of Kid protein in metaphase *Siah1a*$^{-/-}$ spermatocytes or in testis lysates. However *Siah1a*$^{-/-}$ cells that may contain abnormally elevated Kid levels are quickly lost through apoptosis and represent a small fraction of testis cells, which limits their detection by immunofluorescence or Western blotting. Thus we cannot rule out the possibility that Siah1 may facilitate Kid degradation and chromosome segregation during mammalian meiosis I.

Are Siah proteins required for mitosis in vivo? Previous in vitro studies describe Siah1 induction in response to p53 or p21 overexpression (1, 27, 28, 39) and Siah1 repression upon stimulation of growth-arrested cells (24). Furthermore it appears that overexpression of Siah1 is sufficient to arrest cell growth (31), and Siah1 proteins are implicated in p53-mediated β-catenin degradation in response to DNA damage (28, 30, 37). Human SIAH1 overexpression causes mitotic abnormalities and failed cytokinesis, implicating Siah1 proteins in mitosis as well as growth arrest (7). In light of these reports the meiotic cell division phenotype and reduced size of *Siah1a*$^{-/-}$ mice are intriguing. However, several of our findings argue against a

general role for Siah1a in somatic cell growth in vivo. *Siah1a*$^{-/-}$ animals are normal size at birth, and primary fibroblasts derived from *Siah1a*$^{-/-}$ embryos proliferate normally and have normal DNA content. Other rapidly proliferating cells such as those of the gut and hematopoietic system appear unaffected, and, in contrast to what is found for testis germ cells, there is no evidence of increased somatic cell death in *Siah1a*$^{-/-}$ mice.

It is possible that there is considerable functional redundancy among the closely related Siah proteins. Indeed, *Siah2* mutation is synthetically lethal with *Siah1a* mutation, although loss of both genes does not lead to obvious proliferative defects in somatic cells (R. A. Dickins, I. J. Frew, and D. D. L. Bowtell, unpublished observations). Siah1a and Siah1b are almost identical and likely to be biochemically redundant; therefore, *Siah1b* expression may mask the full consequences of Siah1 deficiency. Interestingly, *Siah1b* is on the murine X chromosome, most of which is transcriptionally silenced during meiosis in male germ cells (18). This may explain why removal of *Siah1a* has dire consequences for meiotic but not mitotic cells. Experimental removal of *Siah1b* function will clarify the full repertoire of Siah1 activities.

ACKNOWLEDGMENTS

We are especially grateful to Terry Ashley for providing anti-SCP3 antibodies and advice regarding meiotic prophase analysis. We thank Fiona Christensen for microinjection of blastocysts; Frank Koentgen, Louise Barnett, and Maria Farrell for ES cell suggestions; Mary Thorpe, Kerry Warren, and Alecia Brock-Jones for mouse maintenance; Kerrie Holmes for histology; and Kate Loveland for control reagents. We thank Alex Boussioutas, Sarah Ellis, and Anne O'Connor for assistance with immunohistochemistry, TEM, and hormone assays. Vector pPNT was a kind gift from Paul Orban. We thank Fabien Calvo and Tadashi Yamamoto for providing the anti-Kid antibody and Hironori Funabiki, Patrick Humbert, Matthew O'Connell, and members of the Bowtell lab for suggestions.

This work was supported by grants from the Australian National Health and Medical Research Council to M.K.O., D.M.D.K., and D.D.L.B.

REFERENCES

1. **Amson, R. B., M. Nemani, J. P. Roperch, D. Israeli, L. Bougueleret, I. Le Gall, M. Medhioub, G. Linares-Cruz, F. Lethrosne, P. Pasturaud, L. Piouffre, S. Prieur, et al.** 1996. Isolation of 10 differentially expressed cDNAs in p53-induced apoptosis: activation of the vertebrate homologue of the *Drosophila* seven in absentia gene. Proc. Natl. Acad. Sci. USA **93:**3953–3957.
2. **Antonio, C., I. Ferby, H. Wilhelm, M. Jones, E. Karsenti, A. R. Nebreda, and I. Vernos.** 2000. Xkid, a chromokinesin required for chromosome alignment on the metaphase plate. Cell **102:**425–435.
3. **Baker, S. M., A. W. Plug, T. A. Prolla, C. E. Bronner, A. C. Harris, X. Yao, D. M. Christie, C. Monell, N. Arnheim, A. Bradley, T. Ashley, and R. M. Liskay.** 1996. Involvement of mouse Mlh1 in DNA mismatch repair and meiotic crossing over. Nat. Genet. **13:**336–342.
4. **Boehm, J., Y. He, A. Greiner, L. Staudt, and T. Wirth.** 2001. Regulation of BOB.1/OBF.1 stability by SIAH. EMBO J. **20:**4153–4162.
5. **Boulton, S. J., A. Brook, K. Staehling-Hampton, P. Heitzler, and N. Dyson.** 2000. A role for Ebi in neuronal cell cycle control. EMBO J. **19:**5376–5386.
6. **Brinkley, B. R., S. L. Brenner, J. M. Hall, A. Tousson, R. D. Balczon, and M. M. Valdivia.** 1986. Arrangements of kinetochores in mouse cells during meiosis and spermiogenesis. Chromosoma **94:**309–317.
7. **Bruzzoni-Giovanelli, H., A. Faille, G. Linares-Cruz, M. Nemani, F. Le Deist, A. Germani, D. Chassoux, G. Millot, J. P. Roperch, R. Amson, A. Telerman, and F. Calvo.** 1999. SIAH-1 inhibits cell growth by altering the mitotic process. Oncogene **18:**7101–7109.
8. **Burgoyne, P. S., S. K. Mahadevaiah, M. J. Sutcliffe, and S. J. Palmer.** 1992. Fertility in mice requires X-Y pairing and a Y-chromosomal "spermiogenesis"; gene mapping to the long arm. Cell **71:**391–398.
9. **Carthew, R. W., and G. M. Rubin.** 1990. *seven in absentia*, a gene required for specification of R7 cell fate in the *Drosophila* eye. Cell **63:**561–577.
10. **Chang, H. C., N. M. Solomon, D. A. Wassarman, F. D. Karim, M. Therrien, G. M. Rubin, and T. Wolff.** 1995. phyllopod functions in the fate determination of a subset of photoreceptors in *Drosophila*. Cell **80:**463–472.
11. **Della, N. G., P. V. Senior, and D. D. Bowtell.** 1993. Isolation and characterisation of murine homologues of the *Drosophila* seven in absentia gene (sina). Development **117:**1333–1343.
12. **Dickson, B. J., M. Dominguez, A. van der Straten, and E. Hafen.** 1995. Control of *Drosophila* photoreceptor cell fates by phyllopod, a novel nuclear protein acting downstream of the Raf kinase. Cell **80:**453–462.
13. **Dong, X., L. Tsuda, K. H. Zavitz, M. Lin, S. Li, R. W. Carthew, and S. L. Zipursky.** 1999. ebi regulates epidermal growth factor receptor signaling pathways in *Drosophila*. Genes Dev. **13:**954–965.
14. **Funabiki, H., and A. W. Murray.** 2000. The Xenopus chromokinesin Xkid is essential for metaphase chromosome alignment and must be degraded to allow anaphase chromosome movement. Cell **102:**411–424.
15. **Germani, A., H. Bruzzoni-Giovanelli, A. Fellous, S. Gisselbrecht, N. Varin-Blank, and F. Calvo.** 2000. SIAH-1 interacts with alpha-tubulin and degrades the kinesin Kid by the proteasome pathway during mitosis. Oncogene **19:**5997–6006.
16. **Germani, A., F. Romero, M. Houlard, J. Camonis, S. Gisselbrecht, S. Fischer, and N. Varin-Blank.** 1999. hSiah2 is a new Vav binding protein which inhibits Vav-mediated signaling pathways. Mol. Cell. Biol. **19:**3798–3807.
17. **Heald, R.** 2000. Motor function in the mitotic spindle. Cell **102:**399–402.
18. **Heard, E., and P. Avner.** 2000. Trans-Siberian X press report. International Symposium on X Chromosome Inactivation in Mammals, Institute of Cytology and Genetics, Novosibirsk, Russia, 6–12 September,1999. Trends Genet. **16:**64–65.
19. **Holloway, A. J., N. G. Della, C. F. Fletcher, D. A. Largespada, N. G. Copeland, N. A. Jenkins, and D. D. Bowtell.** 1997. Chromosomal mapping of five highly conserved murine homologues of the *Drosophila* RING finger gene seven-in-absentia. Genomics **41:**160–168.
20. **Hu, G., Y. L. Chung, T. Glover, V. Valentine, A. T. Look, and E. R. Fearon.** 1997. Characterization of human homologs of the *Drosophila* seven in absentia (sina) gene. Genomics **46:**103–111.
21. **Hu, G., and E. R. Fearon.** 1999. Siah-1 N-terminal RING domain is required for proteolysis function, and C-terminal sequences regulate oligomerization and binding to target proteins. Mol. Cell. Biol. **19:**724–732.
22. **Hu, G., S. Zhang, M. Vidal, J. L. Baer, T. Xu, and E. R. Fearon.** 1997. Mammalian homologs of seven in absentia regulate DCC via the ubiquitin-proteasome pathway. Genes Dev. **11:**2701–2714.
23. **Ishikawa, K., S. R. Nash, A. Nishimune, A. Neki, S. Kaneko, and S. Nakanishi.** 1999. Competitive interaction of seven in absentia homolog-1A and Ca2+/calmodulin with the cytoplasmic tail of group 1 metabotropic glutamate receptors. Genes Cells **4:**381–390.
24. **Iyer, V. R., M. B. Eisen, D. T. Ross, G. Schuler, T. Moore, J. C. F. Lee, J. M. Trent, L. M. Staudt, J. Hudson, Jr., M. S. Boguski, D. Lashkari, D. Shalon, D. Botstein, and P. O. Brown.** 1999. The transcriptional program in the response of human fibroblasts to serum. Science **283:**83–87.
25. **Lammers, J. H., H. H. Offenberg, M. van Aalderen, A. C. Vink, A. J. Dietrich, and C. Heyting.** 1994. The gene encoding a major component of the lateral elements of synaptonemal complexes of the rat is related to X-linked lymphocyte-regulated genes. Mol. Cell. Biol. **14:**1137–1146.
26. **Li, S., Y. Li, R. W. Carthew, and Z. C. Lai.** 1997. Photoreceptor cell differentiation requires regulated proteolysis of the transcriptional repressor Tramtrack. Cell **90:**469–478.
27. **Linares-Cruz, G., H. Bruzzoni-Giovanelli, V. Alvaro, J. P. Roperch, M. Tuynder, D. Schoevaert, M. Nemani, S. Prieur, F. Lethrosne, L. Piouffre, V. Reclar, A. Faille, D. Chassoux, J. Dausset, R. B. Amson, F. Calvo, and A. Telerman.** 1998. p21WAF-1 reorganizes the nucleus in tumor suppression. Proc. Natl. Acad. Sci. USA **95:**1131–1135.
28. **Liu, J., J. Stevens, C. A. Rote, H. J. Yost, Y. Hu, K. L. Neufeld, R. L. White, and N. Matsunami.** 2001. Siah-1 mediates a novel beta-catenin degradation pathway linking p53 to the adenomatous polyposis coli protein. Mol. Cell **7:**927–936.
29. **Matsuda, Y., T. Hirobe, and V. M. Chapman.** 1991. Genetic basis of X-Y chromosome dissociation and male sterility in interspecific hybrids. Proc. Natl. Acad. Sci. USA **88:**4850–4854.
30. **Matsuzawa, S., and J. C. Reed.** 2001. Siah-1, SIP, and Ebi collaborate in a novel pathway for beta-catenin degradation linked to p53 responses. Mol. Cell **7:**915–926.
31. **Matsuzawa, S., S. Takayama, B. A. Froesch, J. M. Zapata, and J. C. Reed.** 1998. p53-inducible human homologue of *Drosophila* seven in absentia (Siah) inhibits cell growth: suppression by BAG-1. EMBO J. **17:**2736–2747.
32. **McCarrey, J. R.** 1993. Development of the germ cell, p. 58–89. *In* C. Desjardins, and L. L. Ewing (ed.), Cell and molecular biology of the testis. Oxford University Press, New York, N.Y.
33. **Moens, P. B., and B. Spyropoulos.** 1995. Immunocytology of chiasmata and chromosomal disjunction at mouse meiosis. Chromosoma **104:**175–182.
34. **Nasmyth, K., J. M. Peters, and F. Uhlmann.** 2000. Splitting the chromosome: cutting the ties that bind sister chromatids. Science **288:**1379–1385.
35. **O'Donnell, L., R. I. McLachlan, N. G. Wreford, and D. M. Robertson.** 1994. Testosterone promotes the conversion of round spermatids between stages VII and VIII of the rat spermatogenic cycle. Endocrinology **135:**2608–2614.

36. **Peters, A. H., A. W. Plug, M. J. van Vugt, and P. de Boer.** 1997. A drying-down technique for the spreading of mammalian meiocytes from the male and female germline. Chromosome Res. **5:**66–68.
37. **Polakis, P.** 2001. More than one way to skin a catenin. Cell **105:**563–566.
38. **Relaix, F., X. Wei, W. Li, J. Pan, Y. Lin, D. D. Bowtell, D. A. Sassoon, and X. Wu.** 2000. Pw1/Peg3 is a potential cell death mediator and cooperates with Siah1a in p53-mediated apoptosis. Proc. Natl. Acad. Sci. USA **97:**2105–2110.
39. **Roperch, J. P., F. Lethrone, S. Prieur, L. Piouffre, D. Israeli, M. Tuynder, M. Nemani, P. Pasturaud, M. C. Gendron, J. Dausset, M. Oren, R. B. Amson, and A. Telerman.** 1999. SIAH-1 promotes apoptosis and tumor suppression through a network involving the regulation of protein folding, unfolding, and trafficking: identification of common effectors with p53 and p21(Waf1). Proc. Natl. Acad. Sci. USA **96:**8070–8073.
40. **Russell, L. D., R. A. Ettlin, A. P. Sinha Hikim, and E. D. Clegg.** 1990. Histological and histopathological evaluation of the testis. Cache River Press, Clearwater, Fla.
41. **Sambrook, J., and D. W. Russell.** 2001. Molecular cloning: a laboratory manual, 3rd ed. Cold Spring Harbor Laboratory Press, Cold Spring Harbor, N.Y.
42. **Seifert, H. S., E. Y. Chen, M. So, and F. Heffron.** 1986. Shuttle mutagenesis: a method of transposon mutagenesis for Saccharomyces cerevisiae. Proc. Natl. Acad. Sci. USA **83:**735–739.
43. **Sourisseau, T., C. Desbois, L. Debure, D. D. Bowtell, A. C. Cato, J. Schneikert, E. Moyse, and D. Michel.** 2001. Alteration of the stability of Bag-1 protein in the control of olfactory neuronal apoptosis. J. Cell Sci. **114:**1409–1416.
44. **Sweet, H. O., S. A. Cook, P. Ward-Bailey, and K. R. Johnson.** 1994. Proportional dwarf (pdw), a new recessive mutation on mouse chromosome eight. Mouse Genome **92:**526–528.
45. **Tang, A. H., T. P. Neufeld, E. Kwan, and G. M. Rubin.** 1997. PHYL acts to down-regulate TTK88, a transcriptional repressor of neuronal cell fates, by a SINA-dependent mechanism. Cell **90:**459–467.
46. **Tanikawa, J., E. Ichikawa-Iwata, C. Kanei-Ishii, A. Nakai, S. Matsuzawa, J. C. Reed, and S. Ishii.** 2000. p53 suppresses the c-Myb-induced activation of heat shock transcription factor 3. J. Biol. Chem. **275:**15578–15585.
47. **Tiedt, R., B. A. Bartholdy, G. Matthias, J. W. Newell, and P. Matthias.** 2001. The RING finger protein Siah-1 regulates the level of the transcriptional coactivator OBF-1. EMBO J. **20:**4143–4152.
48. **Tokai, N., A. Fujimoto-Nishiyama, Y. Toyoshima, S. Yonemura, S. Tsukita, J. Inoue, and T. Yamamota.** 1996. Kid, a novel kinesin-like DNA binding protein, is localized to chromosomes and the mitotic spindle. EMBO J. **15:**457–467.
49. **Tybulewicz, V. L., C. E. Crawford, P. K. Jackson, R. T. Bronson, and R. C. Mulligan.** 1991. Neonatal lethality and lymphopenia in mice with a homozygous disruption of the c-abl proto-oncogene. Cell **65:**1153–1163.
50. **Zhang, J., M. G. Guenther, R. W. Carthew, and M. A. Lazar.** 1998. Proteasomal regulation of nuclear receptor corepressor-mediated repression. Genes Dev. **12:**1775–1780.